⌘ *Author's Choice*

THE JOURNAL OF BIOLOGICAL CHEMISTRY VOL. 287, NO. 12, pp. 9429–9440, March 16, 2012

Constitutive Clathrin-mediated Endocytosis of CTLA-4 Persists during T Cell Activation[S]

Received for publication, September 14, 2011, and in revised form, January 10, 2012 Published, JBC Papers in Press, January 19, 2012, DOI 10.1074/jbc.M111.304329

Omar S. Qureshi[‡1], Satdip Kaur[‡2], Tie Zheng Hou[‡3], Louisa E. Jeffery[‡4], Natalie S. Poulter[§], Zoe Briggs[‡3], Rupert Kenefeck[‡], Anna K. Willox[¶], Stephen J. Royle[¶], Joshua Z. Rappoport[§], and David M. Sansom[‡5]

From the [‡]MRC Centre for Immune Regulation, School of Immunity and Infection, University of Birmingham Medical School and [§]School of Biosciences, University of Birmingham, Birmingham B15 2TT and [¶]Physiological Laboratory and Cancer Research UK Centre, University of Liverpool, Crown Street, Liverpool, L69 3BX, United Kingdom

Background: CTLA-4 is an essential regulator of T cell immune responses with unusual intracellular trafficking.
Results: Endocytosis of CTLA-4 is continuous with subsequent recycling and degradation.
Conclusion: Clathrin-mediated endocytosis of CTLA-4 persists in activated T cells.
Significance: This alters our understanding of CTLA-4 behavior and, therefore, how it might function.

CTLA-4 is one of the most important negative regulators of the T cell immune response. However, the subcellular distribution of CTLA-4 is unusual for a receptor that interacts with cell surface transmembrane ligands in that CTLA-4 is rapidly internalized from the plasma membrane. It has been proposed that T cell activation can lead to stabilization of CTLA-4 expression at the cell surface. Here we have analyzed in detail the internalization, recycling, and degradation of CTLA-4. We demonstrate that CTLA-4 is rapidly internalized from the plasma membrane in a clathrin- and dynamin-dependent manner driven by the well characterized YVKM trafficking motif. Furthermore, we show that once internalized, CTLA-4 co-localizes with markers of recycling endosomes and is recycled to the plasma membrane. Although we observed limited co-localization of CTLA-4 with lysosomal markers, CTLA-4 was nonetheless degraded in a manner inhibited by lysosomal blockade. T cell activation stimulated mobilization of CTLA-4, as judged by an increase in cell surface expression; however, this pool of CTLA-4 continued to endocytose and was not stably retained at the cell surface. These data support a model of trafficking whereby CTLA-4 is constitutively internalized in a ligand-independent manner undergoing both recycling and degradation. Stimulation of T cells increases CTLA-4 turnover at the plasma membrane; however, CTLA-4 endocytosis continues and is not stabilized during activation of human T cells. These findings emphasize the importance of clathrin-mediated endocytosis in regulating CTLA-4 trafficking throughout T cell activation.

CTLA-4 is one of the key negative regulators of the immune system as exemplified by the rapid and fatal T cell proliferation observed in CTLA-4 knock-out mice (1, 2). Despite its inhibitory function, CTLA-4 shares two ligands with a stimulatory cell surface receptor CD28 (3), raising questions as to how ligand engagement can precisely direct both stimulatory and inhibitory outcomes.

CTLA-4 inhibition has been widely considered to derive from a T cell-intrinsic inhibitory signal (4, 5) resulting from binding to its cell surface ligands. However, several alternate possibilities have been suggested. Importantly, an increasing number of studies have indicated that CTLA-4 is also capable of cell-extrinsic inhibition or suppression of T cell responses, and *in vivo* it appears that a cell-extrinsic mechanism is likely to be the most significant in preventing autoimmunity (6, 7). We recently proposed a cell-extrinsic mechanism for CTLA-4 that involves the capture or "trans-endocytosis" of co-stimulatory molecules on antigen-presenting cells that then functions by depriving T cells of CD28-mediated co-stimulation (8). Given the potential importance of CTLA-4 trafficking to such functions, we have re-evaluated a number of key concepts associated with CTLA-4 expression patterns to allow us to better relate these features to its proposed mechanisms of action.

It is well accepted that in contrast to CD28, which is expressed robustly at the cell surface, CTLA-4 has a largely intracellular distribution that is dependent on motifs contained within the C terminus of CTLA-4 (9–12). T cell activation is then thought to deliver CTLA-4 to the cell surface from an intracellular compartment (10, 13–16) in a manner that may be proportional to the intensity of T cell receptor signaling (17). However, the fate of CTLA-4 subsequent to T cell receptor-driven up-regulation is not well understood. Previous biochemical studies have clearly shown an interaction of CTLA-4 with the clathrin adaptor adaptor protein-2 (AP-2)[6] and, accordingly, mutations within the CTLA-4 tyrosine-based $YXX\phi$ motif inhibit internalization (18). One attractive possibility is, therefore, that this motif is phosphorylated in response to T cell activation by src kinases, which might then lead to the stabilization of CTLA-4 at the plasma membrane (19–22). Such sta-

⌘ *Author's Choice*—Final version full access.
[S] This article contains supplemental Fig. S1.
[1] Supported by the Biotechnology and Biological Sciences Research Council, Swindon, United Kingdom.
[2] Supported by an Medical Research Council Ph.D. studentship.
[3] Supported by the Wellcome Trust (Grant 092578).
[4] Supported by Arthritis Research UK.
[5] To whom correspondence should be addressed. Tel.: 44-121-414-2268; E-mail: D.M.Sansom@bham.ac.uk.

[6] The abbreviations used are: AP-2, adaptor protein-2; RFP, red fluorescent protein; TIRF, total internal reflection fluorescence; CHX, cycloheximide; PE, phosphatidylethanolamine; PMA, phorbol 12-myristate 13-acetate; APC, antigen presenting cell.

bilization could be important for an inhibitory signal as ordinarily CTLA-4 surface levels are low. However, because increases in CTLA-4 surface expression may result from increased protein synthesis, enhanced delivery to the plasma membrane, or decreased internalization, we sought to define more clearly the basic mechanisms of CTLA-4 trafficking and the effect of T cell activation on this behavior.

Using model systems of CTLA-4 trafficking as well as human T cells, we observed that CTLA-4 was efficiently internalized via a clathrin- and dynamin-dependent route independent of ligand binding. Once internalized, CTLA-4 was found to be both recycled and degraded. In T cells, CTLA-4 was mobilized to the cell surface upon stimulation but not stabilized at the plasma membrane. Instead, CTLA-4 continued to undergo endocytosis, recycling, and degradation, suggesting that these features are part of the normal physiology of CTLA-4 function.

EXPERIMENTAL PROCEDURES

DNA Constructs and Transfectants

Full-length CTLA-4 cDNA was cloned into a CMV expression vector pcDNA3.1 as previously described (15). CTLA-4 constructs with either the last 13 or last 23 amino acids deleted were generated by PCR and cloned into the same vector. Point mutation of CTLA-4 Y201A was generated using QuikChange Mutagenesis Kit II (Agilent Technologies). shRNA targeting AP-2 and co-expressing RFP were purchased from Origene. Plasmids expressing mCherry-tagged Eps15 or Eps15 EH29 were made by exchanging mCherry for GFP using NheI-BsrGI sites in GFP-tagged versions of these plasmids (23). RFP-tagged rat endophilin constructs in pcDNA3.1 were gifts from Leon Lagnado. mCherry-AP180-C was made as described (24). Dominant-negative effects of constructs on clathrin-mediated endocytosis were validated by inhibition of transferrin uptake. DsRed-tagged Rab constructs were from Addgene and were generated by Sharma *et al.* (25).

Cell Purification and Culture

CHO Cell Lines—CHO cell lines expressing different DNA constructs were generated by electroporation of human cDNAs cloned into a CMV expression vector. Cells were grown in DMEM containing 10% FBS. Cells expressing the plasmid were selected using G418 (500 μg/ml) treatment and by cell sorting. Cultures were maintained at 37 °C in a humidified incubator containing 5% CO_2 and were passaged by trypsinization.

T Cells—For CD4+CD25− T cell isolation, peripheral blood mononuclear cells were isolated from fresh buffy coats (provided by the National Blood Transfusion Service, Birmingham, UK) using Ficoll-Paque density centrifugation. $CD4^+$ T cells were isolated by incubating peripheral blood mononuclear cells with human $CD4^+$ T cell-enrichment mixture with an additional anti-CD25 depletion antibody and magnetic colloid according to the manufacturer's instructions (Stem Cell Technologies). Where indicated, cells were stimulated with 50 ng/ml PMA and 1 μM ionomycin or anti-CD3 anti-CD28 Dynabeads (Invitrogen). T cell blasts were generated by stimulation with anti-CD3 anti-CD28 Dynabeads for 3–7 days.

Confocal Microscopy

Imaging was carried out using a Zeiss LSM 510 or a Zeiss LSM 780 inverted laser scanning confocal microscope using a 100× oil immersion objective with excitation at 488, 543, and 633 nm. Constant laser powers and acquisition parameters were maintained throughout individual experiments for analysis. For live-cell imaging, Z-stacks were acquired every minute. Digital images were prepared using ImageJ (Wayne Rasband, NIH). For quantitation, cells were outlined, and mean fluorescence intensity was measured using ImageJ. All confocal images shown are representative of at least 30 micrographs taken from at least three independent experiments.

Immunofluorescence Staining—For analysis of surface *versus* internalized CTLA-4, CHO cells expressing CTLA-4 were plated overnight on a poly-L-lysine-coated coverslip in a 24-well plate. Where indicated, cells were transfected with the indicated DNA constructs (AP180CGFP, GFP, dynamin K44A RFP, dynamin RFP). Cells were then incubated with unconjugated anti-CTLA-4 (clone 11G1) for 30 min. Cells were then washed 3 times with medium (4 °C) and placed on ice. Surface receptors were labeled on ice by the addition of Alexa488-, 555-, or 647-conjugated anti-mouse IgG. Cells were then washed with 4 °C media, fixed with 3% paraformaldehyde in PBS, and permeabilized with PBS containing 0.1% saponin (PBS/sap). Internalized receptors were then detected by incubation with PBS/sap containing Alexa488-, 555- or 647-conjugated anti-mouse IgG. After staining, coverslips were dried and mounted with Vectashield (Vector Laboratories) before visualization by confocal microscopy.

Dynasore—For dynasore treatment, cells were labeled with a far-red dye (DDAO-SE, Invitrogen) as previously described (8). Cells were then preincubated in serum-free medium containing 80 μM dynasore for 30 min. Anti-CTLA-4 PE (BD Biosciences) was then added for 30 min, and cells were transferred to glass-bottom dishes (MatTek) for imaging by confocal microscopy.

Total Internal Reflection Fluorescence (TIRF) Microscopy Image Acquisition—TIRF images were acquired on a Nikon EclipseTi inverted microscope TIRF system, which uses high numerical aperture objective-based TIRF with the laser light being delivered to the sample through the objective (CFI TIRF Apo 60× oil NA 1.49, Nikon). Adherent CHO cells expressing CTLA-4 and clathrin light chain GFP were fixed and surface CTLA-4-labeled with anti-CTLA-4 Alexa555. The 488-nm line of an argon ion 457–514-nm laser was used to image the clathrin-GFP, and the green diode 561-nm laser was used to image the Alexa-568-labeled CTLA-4. Images were captured on a 14-bit CCD camera (Andor iXon 1M EMCCD DU885) using Nikon NIS Elements software with exposure times of 600 ms (green) and 500 ms (red).

Co-localization—For Rab11 co-localization, CHO cells expressing CTLA-4 were co-transfected with Rab11 DsRed (Addgene) (26) and plated on glass-bottom dishes overnight. Cells were then imaged by confocal microscopy. For LAMP-1 co-localization, HeLa cells expressing CTLA-4 were plated on PLL-coated coverslips overnight, fixed with paraformaldehyde 3%, permeabilized with PBS/sap, and stained using anti-

LAMP-1 (Abcam) and anti-CTLA-4 (SantaCruz) primary antibodies. Subsequently cells were stained with Alexa488-conjugated anti-mouse IgG and Alexa555-conjugated anti-goat IgG before mounting and visualization by confocal microscopy.

Recycling Assay—CHO cells expressing CTLA-4 were plated on poly-L-lysine-coated coverslips overnight. Cells were then labeled with unconjugated anti-CTLA-4 (11G1, a gift from J. Allison) for 1 h. Cells were then washed and incubated at 4 °C with Alexa488-conjugated anti-mouse secondary antibody to label any surface receptors. Cells were then warmed to 37 °C and incubated with Alexa555-conjugated anti-mouse secondary antibody to label recycling receptors. To check that surface receptors were fully blocked, Alexa555-conjugated secondary was also applied to cells at 4 °C.

For live-cell imaging of receptor cycling, cells were incubated for 60 min with Alexa488-conjugated anti-CTLA-4. Cells were then washed and incubated for 5 min at 37 °C. Alexa-555 secondary antibody was then added, and cells were visualized at 37 °C by confocal microscopy in the presence of the antibody.

Flow Cytometry Assays

Flow cytometry was carried out using a Dako Cyan flow cytometer and acquired using Summit software. Compensation and analysis was performed using FlowJo (TreeStar). Flow cytometric plots are representative of at least three independent experiments.

For analysis of surface-to-cycling ratios CTLA-4, cells were first incubated with anti-CTLA-4 PE (BD Biosciences) for 30 min at 37 °C. Cells were then placed on ice and washed 3 times with 4 °C medium. Surface CTLA-4 was then labeled by incubation on ice with Alexa633 anti-mouse secondary antibody. Cells were then washed and analyzed by flow cytometry.

For analysis of surface CTLA-4 staining in the presence of dominant negative constructs, CHO cells expressing CTLA-4 were transfected and 24 h later labeled on ice with PE- or APC-conjugated anti-CTLA-4.

For analysis of cycling to total CTLA-4, cells were labeled at 37 °C with anti-CTLA-4 PE. Cells were then fixed, permeabilized with PBS/sap, and labeled with anti-CTLA-4 (C19 Santa Cruz Biotechnology) and Alexa633-conjugated anti-goat secondary antibody.

Western Blotting

A total of 4×10^6 cells suspended in 5 ml of medium alone or medium supplemented with cycloheximide (CHX), NH_4Cl, or both CHX and NH_4Cl were incubated at 37 °C for 3 h. Cells were pelleted and lysed in 1 ml of 1% Triton X-100 (1% Triton, 20 mM Tris, pH 7.5, 150 nM NaCl, 1 mM EDTA, and 0.02% sodium azide) at 4 °C for 30 min containing protease mixture inhibitor (1:100). Immunoprecipitation of CTLA-4 was performed with anti-human CTLA-4 antibody coupled to protein G beads at 4 °C for 1.5 h. Beads were then washed extensively in lysis buffer and resuspended in 40 μl of Protein Loading Buffer (2×). Proteins were analyzed by sodium dodecyl sulfate polyacrylamide gel electrophoresis and Western blotting.

RESULTS

CTLA-4 Endocytosis Is Constitutive and Independent of Ligand Binding—The cytoplasmic domain of CTLA-4 contains 36 amino acids that control its intracellular trafficking itinerary. Interaction of the tyrosine-based motif (YVKM) with AP-2 has been determined biochemically, and CTLA-4 internalization is reported to utilize this motif (9, 18, 21). Using CHO cell lines expressing truncations of the CTLA-4 C terminus (Fig. 1*A*), we assessed the internalization of these CTLA-4 variants from the plasma membrane. To assay internalization, we pulsed cells at 37 °C for 30 min with an unlabeled anti-CTLA-4 to mark all the CTLA-4 protein cycling via the plasma membrane. We then placed cells on ice to stop trafficking and detected labeled CTLA-4 remaining at the cell surface with a secondary antibody (*red*). Subsequently, the cells were fixed, permeabilized, and stained for labeled intracellular CTLA-4 with an alternate secondary antibody (*green*) before analyzing cells by confocal microscopy (Fig. 1*B*). The ratio of surface (*red*) to internalized (*green*) CTLA-4 staining was calculated as described under "Experimental Procedures" and gives a measure of endocytosis (Fig. 1*B*). As predicted, cells expressing deletions of the CTLA-4 C terminus that removed the YVKM motif demonstrated highly impaired endocytosis.

To assay the efficiency of CTLA-4 internalization by flow cytometry, a directly conjugated (PE-labeled) anti-CTLA-4 antibody was incubated with cells at 37 °C to detect CTLA-4 that trafficked via the plasma membrane during a 30-min period. This CTLA-4 pool (cycling CTLA-4) labeled at the plasma membrane included surface receptors and those that subsequently internalized. To specifically detect those receptors that remained at the cell surface, the cells were subsequently labeled at 4 °C with an Alexa633-conjugated secondary antibody (Fig. 1*C*). For the non-endocytic Δ23 mutant, which lacks the YVKM motif, a linear relationship was observed between the staining at 37 °C (cycling) and the staining at 4 °C (surface) (Fig. 1*D*, *red line*). This was expected as those receptors labeled with anti-CTLA-4 at 37 °C remain at the cell surface and are, therefore, available for labeling by the Alexa633 secondary antibody at 4 °C. In contrast, both WT and Δ13 deviated substantially from this relationship such that less cell surface CTLA-4 was detected for the equivalent amount of CTLA-4 labeling. This is indicative of an endocytic receptor as the labeling of CTLA-4 at 37 °C allows internalization of CTLA-4 that cannot be subsequently detected by incubation with secondary antibody at 4 °C. This result also clearly contrasted with the linear relationship observed when this assay was performed with CD28 (Fig. 1*E*). Furthermore, mutation of the YVKM motif to AVKM demonstrated directly that this motif controls endocytosis (Fig. 1*E*). These data, therefore, provide clear evidence that the cytoplasmic domain of CTLA-4 (specifically the YVKM motif) controls internalization from the plasma membrane.

To determine the rate of internalization, we labeled cells at 4 °C with anti-CTLA-4 to detect surface CTLA-4. We then warmed the cells to 37 °C for various time points and detected the fraction of the initial label that remained at the cell surface (Fig. 1*F*). As expected, this indicated the internalization of

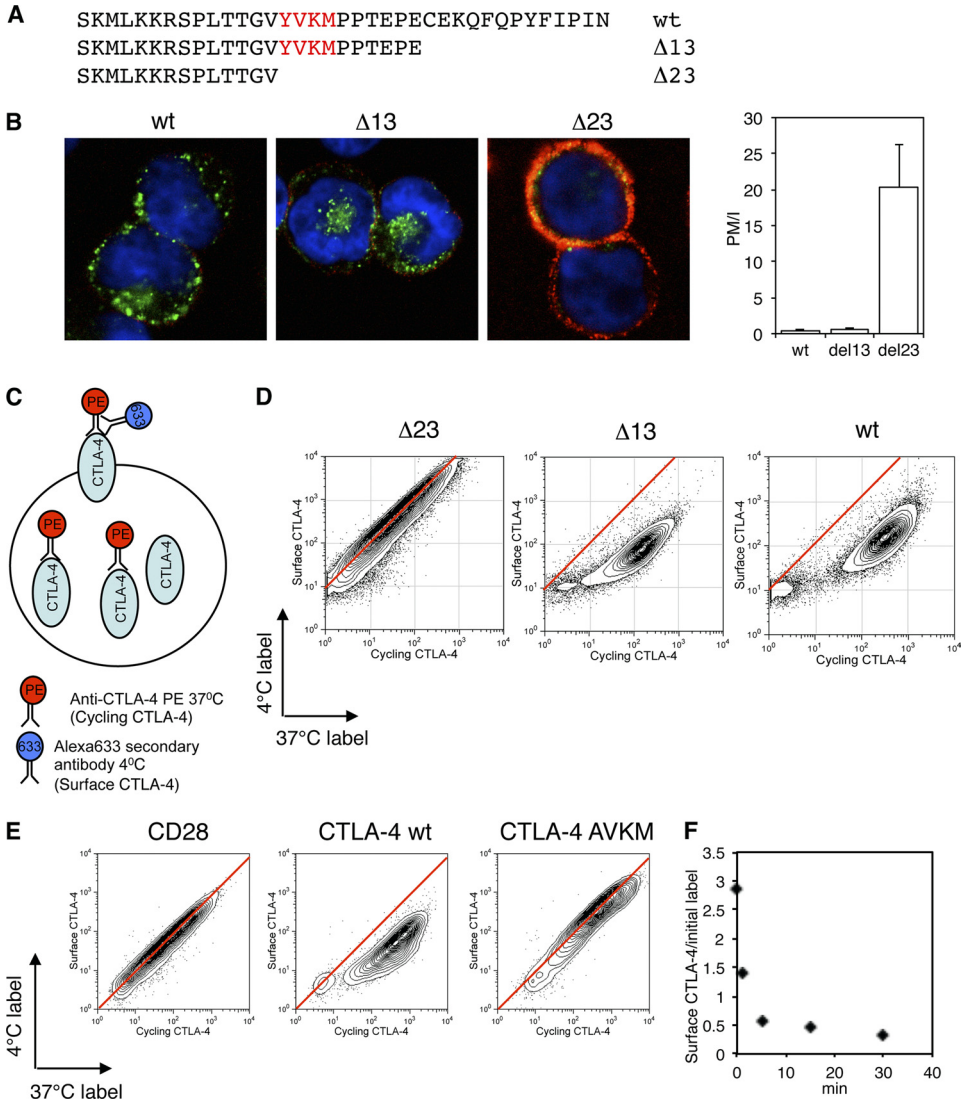

FIGURE 1. **Endocytosis of CTLA-4.** *A*, CTLA-4 C-terminal sequence alignments show the truncations used in this study. *B*, CHO cells expressing either wild type (*wt*), Δ13, or Δ23 CTLA-4 were incubated with unlabeled anti-CTLA-4 at 37 °C for 30 min. Cells were then cooled to 4 °C, and CTLA-4 that remained on the cell surface were stained with a fluorescently labeled secondary antibody (*red*). Cells were then fixed, permeabilized, and stained with a different secondary antibody (*green*) and imaged by confocal microscopy. The ratio of plasma membrane to internalized CTLA-4 fluorescence (PM/I) was calculated by outlining cells in ImageJ and is shown in the *right panel*. *C*, diagram of the antibody labeling strategy for flow cytometry experiments in *D* and *E*. *D*, CHO cells expressing different CTLA-4 truncations were labeled with anti-CTLA-4 PE at 37 °C for 30 min followed by labeling surface CTLA-4 on ice (4 °C) with a fluorescently conjugated anti-mouse secondary antibody. Cells were analyzed by flow cytometry. *E*, CHO cells expressing CD28, CTLA-4 wt, or CTLA-4 AVKM were labeled as described in *C* and *D* and analyzed by flow cytometry. *Red lines* indicate the staining ratio of Δ23 (*D*) or CD28 (*E*) as a guide for the expected ratio for a cell surface protein. *F*, CHO cells expressing wild-type CTLA-4 were labeled at 4 °C with anti-CTLA-4 PE to label surface CTLA-4. Cells were then warmed to 37 °C for the time indicated, and CTLA-4 remaining on the surface was detected on ice with a fluorescently conjugated anti-mouse secondary antibody. The time course of surface labeling is plotted against initial labeling.

CTLA-4 was rapid, with the majority of surface CTLA-4 internalizing within 5 min. Together these data show that in CHO cell lines CTLA-4 is rapidly internalized in a ligand-independent manner via its YVKM motif, contrasting with the constitutive surface expression of CD28.

Internalization of CTLA-4 Utilizes a Clathrin- and Dynamin-sensitive Pathway—Endocytosis of proteins can be mediated by a number of mechanisms including both clathrin-dependent endocytosis as well as a number of clathrin-independent pathways. Although the control of CTLA-4 endocytosis by the YVKM endocytic motif is known, the use of clathrin and dynamin has not been well established. To test these pathways directly, we initially incubated CHO-CTLA-4 cells with anti-CTLA-4 in the presence of the dynamin inhibitor dynasore (27). As shown in Fig. 2*A*, in control cells, anti-CTLA-4 was internalized into vesicles at 37 °C, whereas in dynasore-treated cells it remained at the cell surface, although still in puncta. We repeated this experiment in a more quantitative manner using flow cytometry, and the relationship of surface to cycling CTLA-4 was tested as in Fig. 1. In the presence of dynasore, the relationship between surface and cycling CTLA-4 was again essentially linear, indicating that inhibiting dynamin caused CTLA-4 to remain at the cell surface (Fig. 2*B*). In an independent approach we also expressed an RFP-tagged dominant-negative inhibitor of dynamin (dynamin K44A) and assayed surface CTLA-4 expression by flow cytometry. This revealed

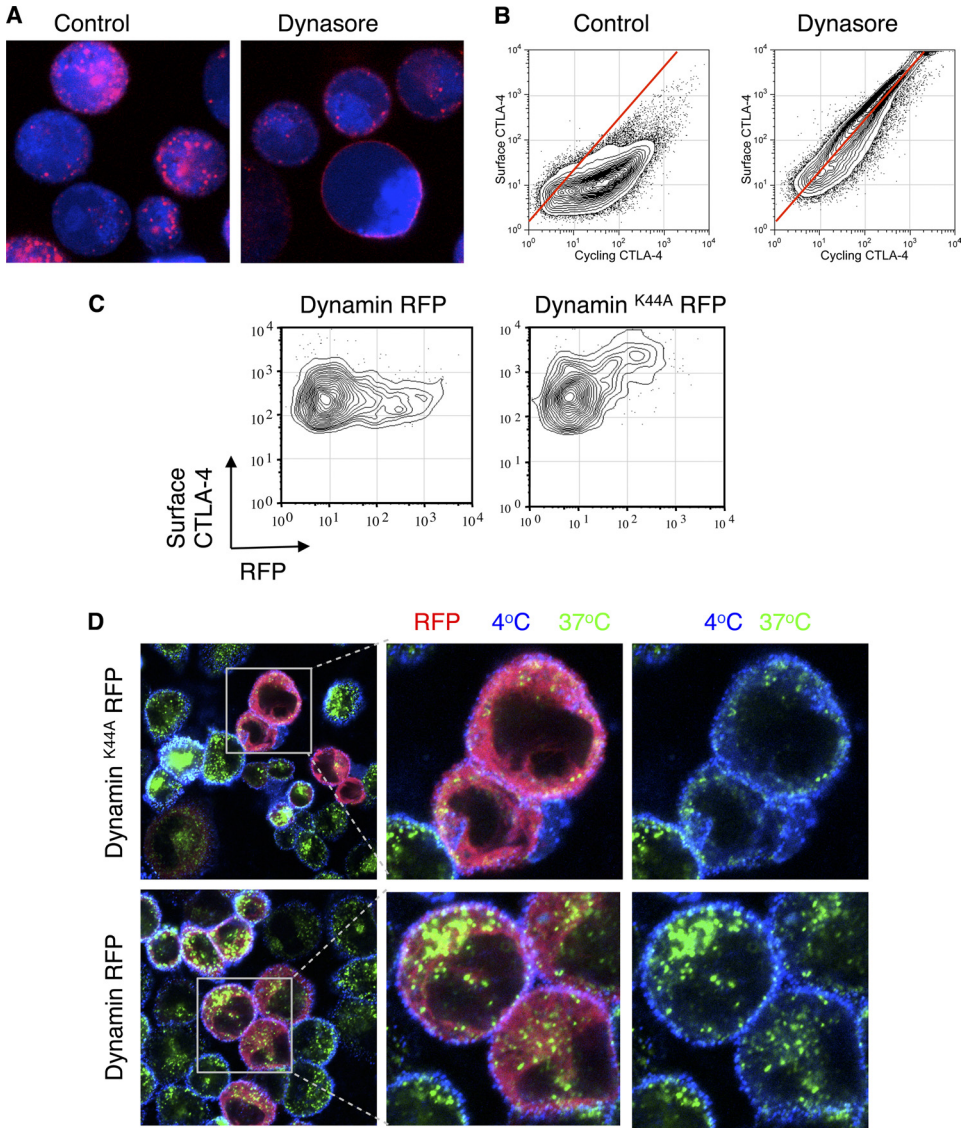

FIGURE 2. **Dynamin-dependent endocytosis of CTLA-4.** *A*, CHO cells expressing CTLA-4 were dye-labeled (*blue*) and preincubated with dynasore (80 μM) for 30 min. Cells were then incubated with anti-CTLA-4 PE (*red*) at 37 °C in the presence of 80 μM dynasore for 30 min. *B*, CHO cells expressing CTLA-4 were labeled with anti-CTLA-4 PE at 37 °C for 30 min in the presence or absence of dynasore followed by labeling of surface CTLA-4 on ice with a fluorescently conjugated anti-mouse secondary antibody and analyzed by flow cytometry. *C*, CHO cells expressing CTLA-4 were transfected with either dynamin K44A RFP or dynamin RFP. Surface CTLA-4 was then labeled on ice using an anti-CTLA-4 APC conjugate and detected by flow cytometry. *D*, cells as described in *C* were incubated with unconjugated mouse anti-CTLA-4 for 30 min at 37 °C. Cells were then cooled to 4 °C, and receptors remaining at the cell surface were stained using an anti-mouse Alexa647 antibody (*blue*). Cells were fixed/permeabilized, and internalized receptors were stained with an anti-mouse Alexa555 antibody (*green*). Cells were analyzed by confocal microscopy.

that in those cells expressing dynamin K44A (RFP+ cells) there was a corresponding increase in surface expression compared with those expressing WT dynamin RFP (Fig. 2*C*). Confocal microscopy (Fig. 2*D*) also confirmed inhibited endocytosis and the predominantly plasma membrane expression of CTLA-4 in the presence of dynamin inhibition.

To test a role for clathrin in CTLA-4 endocytosis, we transfected CHO cells expressing CTLA-4 with a GFP-tagged clathrin construct and visualized cells by TIRF microscopy to observe receptors at or within 100 nm of the cell surface (Fig. 3*A*). This revealed co-localization of CTLA-4 puncta with clathrin, implicating a role for clathrin in CTLA-4 endocytosis. In addition, we transfected cells with the GFP-tagged C terminus of AP180 (AP180C), which acts as a dominant-negative inhibitor of clathrin-mediated endocytosis, and assayed surface CTLA-4 expression. This revealed that in those cells expressing AP180C (GFP+) there was a corresponding increase in CTLA-4 surface expression (Fig. 3*B*). We also carried out confocal microscopy which again demonstrated inhibited endocytosis and increased plasma membrane expression of CTLA-4 as shown by increased co-localization of 4 °C and 37 °C staining (*cyan*, Fig. 3*C*). Quantification of these images demonstrated an increase in the plasma membrane/intracellular ratio by AP180C (Fig. 3*D*). Together these data support a role for clathrin-mediated endocytosis in controlling CTLA-4 surface expression. Overexpression of other components of the clathrin-mediated endocytic pathway, including EPS15, endophilin, and Eps15 EH29, also had an inhibitory effect on endocytosis and increased surface expression of CTLA-4, highly consistent with a role for clathrin in CTLA-4 endocytosis (Fig. 3*E*).

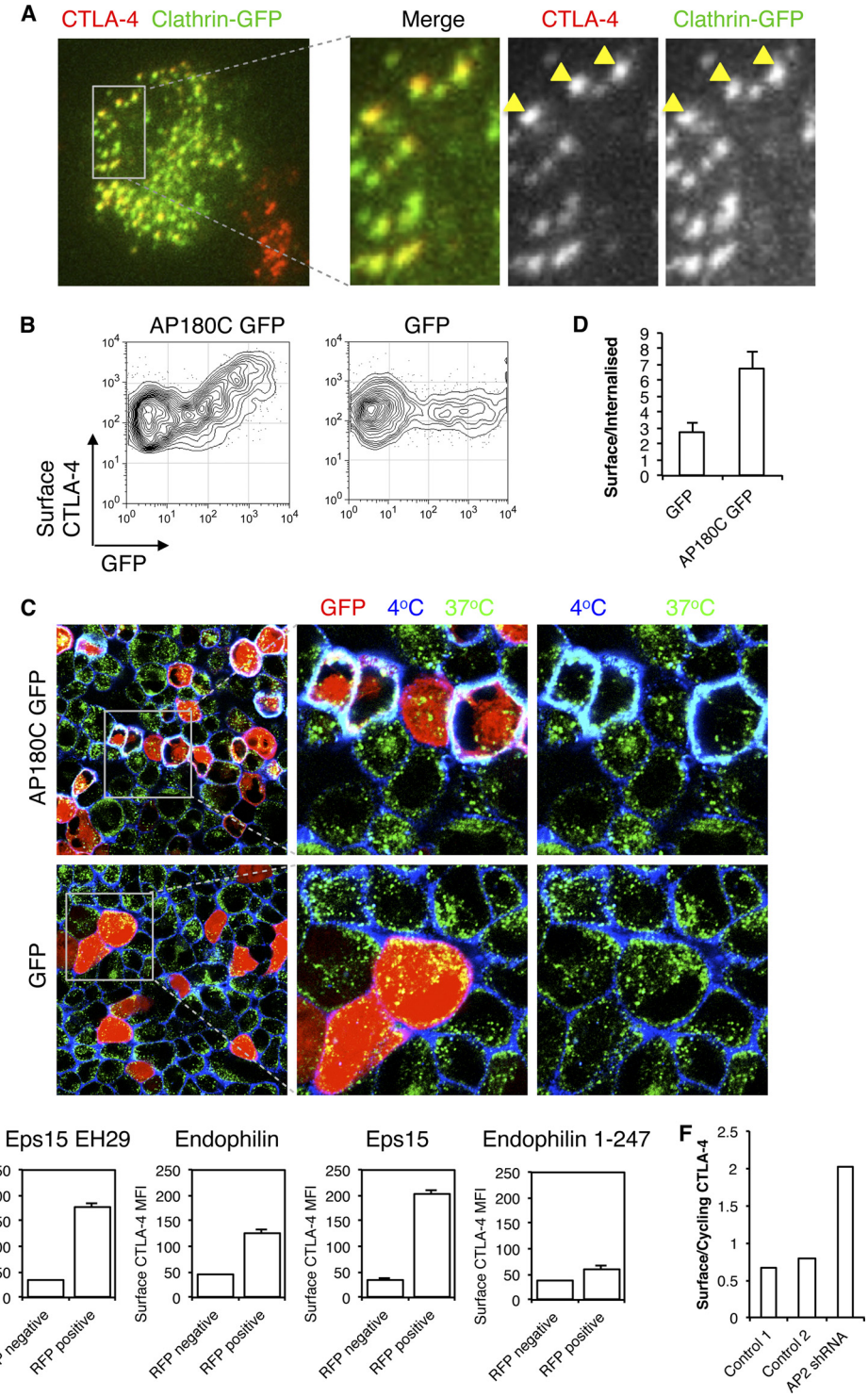

FIGURE 3. **Clathrin-dependent endocytosis of CTLA-4.** *A*, CHO cells expressing CTLA-4 were transfected with GFP-tagged clathrin light chain (*green*). Cells were fixed and surface CTLA-4-labeled with anti-CTLA-4 Alexa546 (*red*). Cells were then analyzed by TIRF microscopy for co-localization of CTLA-4 and clathrin (*yellow*). *B*, CHO cells expressing CTLA-4 were transfected with either AP180C-GFP or unfused-GFP. Cells were then stained for surface CTLA-4 at 4 °C with anti-CTLA-4 PE and analyzed by flow cytometry. *C*, cells in *B* were incubated with unconjugated mouse anti-CTLA-4 for 30 min at 37 °C. Cells were then cooled to 4 °C, and receptors remaining at the cell surface were stained using an anti-mouse Alexa647 antibody (*blue*). Cells were then fixed and permeabilized, and internalized receptors were stained with an anti-mouse Alexa555 antibody (*green*). Cells were analyzed by confocal microscopy for colocalization (*cyan*). *Right panels* show enlargements of the *boxed area*. *D*, the graph shows the ratio of surface to internalized CTLA-4 fluorescence quantified from confocal images stained as in C. *E*, CHO cells expressing CTLA-4 (CHO CTLA-4) were transfected with RFP-tagged dominant negative inhibitors of clathrin-mediated endocytosis, and surface CTLA-4 expression was analyzed by flow cytometry by gating on RFP+ and RFP− cells from the same culture. *F*, CHO CTLA-4 were transfected with shRNA against the μ2 subunit of AP-2 or control shRNA constructs. Cells were labeled with anti-CTLA-4 PE at 37 °C followed by labeling surface CTLA-4 with anti-mouse 647 at 4 °C. The graph shows the ratio of surface CTLA-4 to cycling CTLA-4.

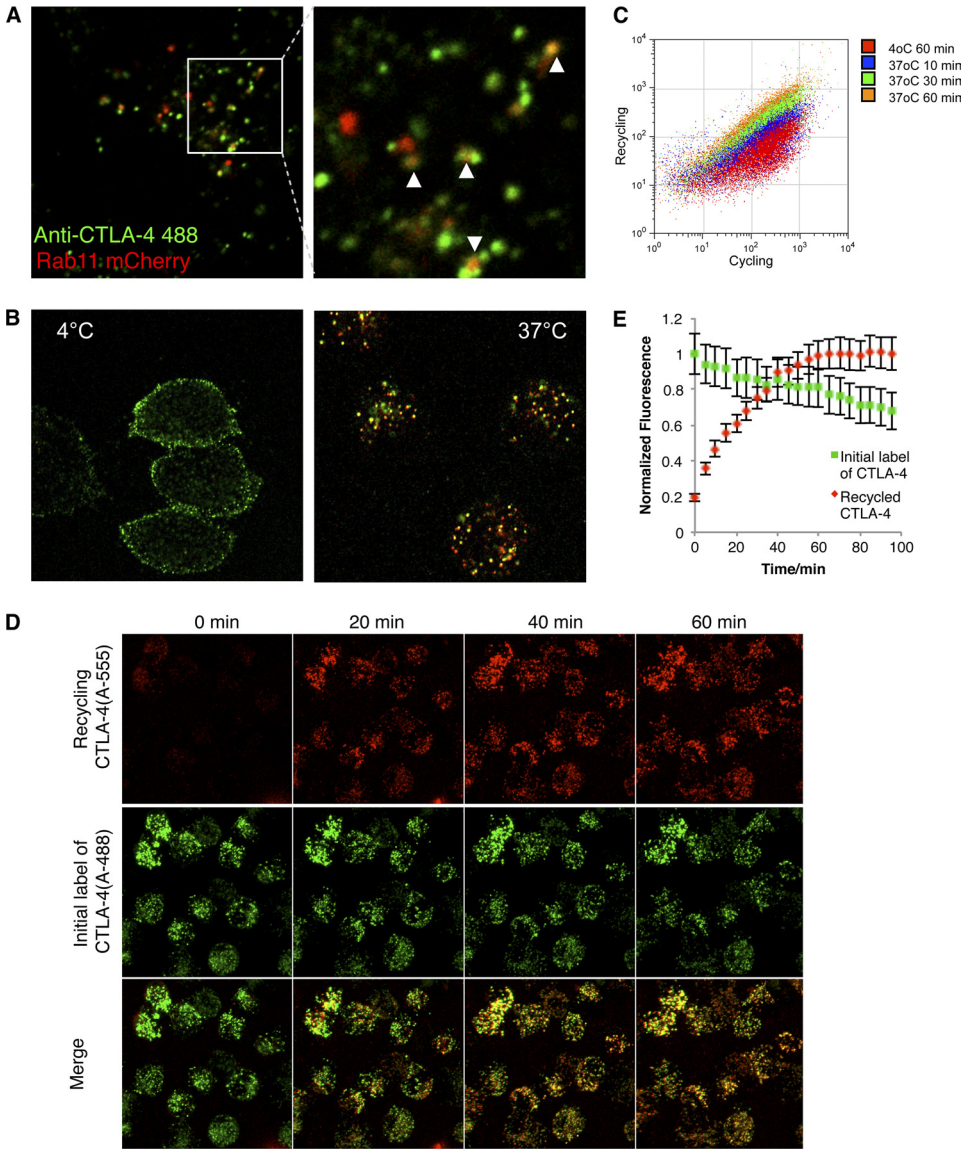

FIGURE 4. **Internalized CTLA-4 recycles to the plasma membrane.** *A*, CHO cells expressing CTLA-4 were transfected with Rab11-mCherry (*red*). Cells were then incubated with Alexa488-conjugated anti-CTLA-4 (*green*) for 30 min at 37 °C and observed by confocal microscopy. The *white arrowheads* indicate co-localization. *B*, CHO cells expressing CTLA-4 were labeled for 1 h with unconjugated mouse anti-CTLA-4. Cells were then placed on ice and surface CTLA-4-labeled with Alexa488 anti-mouse IgG (*green*). To observe recycling receptors, cells were then washed and labeled with Alexa555 anti-mouse IgG (*red*) at 37 °C for 45 min and fixed before confocal analysis. Control conditions are shown (*left*) where the Alexa555 antibody was incubated at 4 °C compared with incubation at 37 °C (*right*). *C*, flow cytometric analysis of recycling CTLA-4 is shown. Cells were labeled with mouse anti-CTLA-4 PE at 37 °C to detect cycling CTLA-4, which was followed by labeling of re-cycling protein with Alexa647 anti-mouse IgG at 4 or 37 °C for the indicated time-points. *D*, live-cell confocal imaging of recycling receptors was carried out using CTLA-4-expressing CHO cells. Cells were incubated with Alexa488-conjugated anti-CTLA-4 for 1 h at 37 °C. Cells were then washed, and surface CTLA-4 receptors were blocked with unconjugated anti-human IgG. Cells were then incubated with Alexa555-conjugated anti-human IgG to detect recycling receptors. Confocal Z-stacks were then acquired at the time points shown. *Panel E* shows quantification of cells from *D*. Cells were outlined in Image J, and the recycling mean pixel fluorescence is plotted against time. *Error bars* show S.E.

Finally to specifically test the role of AP-2, we incubated CTLA-4-transfected cells with an shRNA construct against the μ2 subunit of AP-2 in a vector that also expressed RFP. Cells were gated on RFP expression, and surface CTLA-4 was plotted against cycling CTLA-4. In cells expressing the highest level of the RFP vector we observed a reduction in endocytosis as judged by the ratio of surface to cycling CTLA-4 (Fig. 3*F*). Together, these results demonstrated that in intact cells, CTLA-4 surface expression is controlled by AP-2, dynamin, and clathrin-mediated endocytosis.

CTLA-4 Is Recycled after Internalization—To sustain a continuous cycling pool of CTLA-4, cells must either constitutively synthesize new protein or recycle endocytosed receptors. We, therefore, sought to test the contribution of recycling and degradation pathways to CTLA-4 homeostasis. A proportion of internalized CTLA-4 co-localized with the recycling endosome marker Rab11 (Fig. 4*A*) along with some co-localization with the endosomal markers Rab5, Rab7, and Rab9 (supplemental Fig. 1). We, therefore, investigated the possibility that CTLA-4 could recycle after internalization. To directly establish whether internalized CTLA-4 returned to the plasma membrane, we incubated cells with an unlabeled anti-CTLA-4 at 37 °C for 1 h to label the cycling pool of CTLA-4. We then placed the cells on ice and labeled any remaining cell surface

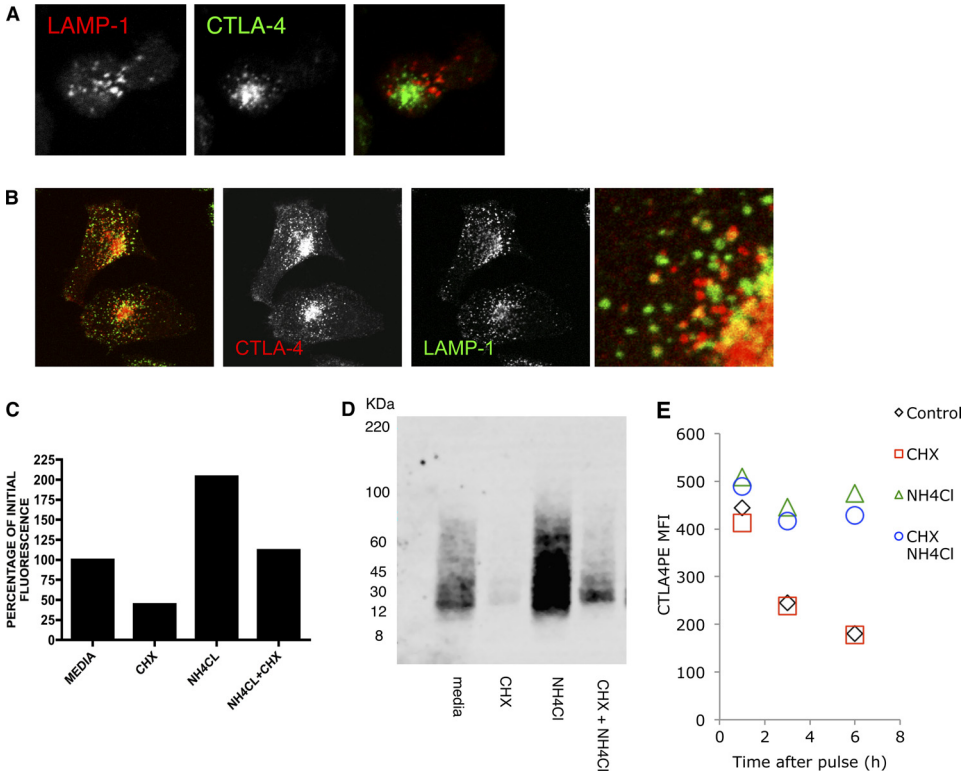

FIGURE 5. **Degradation of CTLA-4 in lysosomal compartments.** *A*, human primary T cell blasts were fixed and stained for CTLA-4 (*green*) and LAMP-1 (*red*) and imaged by confocal microscopy. *B*, HeLa cells transfected with CTLA-4 were fixed and stained for CTLA-4 (*red*) and anti-human LAMP-1 (*green*) and imaged by confocal microscopy. The *right panel* shows an enlarged image. *C*, CHO cells expressing CTLA-4 were treated as shown for 3 h followed by fixation and staining for total cellular CTLA-4 using anti-CTLA-4 PE. Cells were analyzed by flow cytometry, and the relative fluorescence was plotted. *D*, CHO-CTLA-4 cells were incubated in the presence of CHX or ammonium chloride (NH_4Cl) for 3 h. CTLA-4 was then immunoprecipitated, and expression was analyzed by Western blotting. *E*, CHO-CTLA-4 cells were labeled with a 1-h pulse of anti-CTLA-4 PE. Cells were then washed and incubated for various time-points in the presence or absence of CHX and/or NH_4Cl and analyzed for CTLA-4 expression by flow cytometry.

CTLA-4 green using an Alexa488-conjugated secondary antibody. Cells were then further stained at 37 °C with an Alexa 555-conjugated secondary antibody. This detects any recycling receptors that were inaccessible to the initial Alexa488 secondary but that then subsequently recycle to the plasma membrane, labeling them red. Control stains at 4 °C did not show any additional red surface labeling with the Alexa555 secondary at 4 °C (Fig. 4*B*, *left panel*). In contrast, labeling at 37 °C revealed a clear population of recycling CTLA-4 receptors (Fig. 4*B*, *right*). These observations were supported by flow cytometry of bulk cell populations that also showed increasing labeling of cells with a secondary antibody over time (Fig. 4*C*). Additional kinetics of CTLA-4 recycling was also carried out by confocal microscopy. Cells were incubated with Alexa488-conjugated anti-CTLA-4 for 1 h and then imaged over time by confocal microscopy in the presence of an Alexa555-conjugated secondary antibody at 37 °C (Fig. 4*D*). This revealed a steady increase in Alexa555-labeled (re-cycling) CTLA-4 that increased in intensity for ~60 min (Fig. 4*E*). We also observed a steady decline in Alexa488, suggesting some CTLA-4 degradation. Together these data illustrate the dynamic nature of CTLA-4 trafficking in which internalized receptors are recycled to the plasma membrane.

CTLA-4 Is Degraded in Lysosomes—CTLA-4 has been reported to be delivered to the cell surface from secretory lysosomes; however, its relatively short half-life makes it questionable whether this would be a storage compartment of the receptor. In primary T cells we observed little co-localization of CTLA-4 with the lysosomal marker LAMP-1, suggesting it was not stored in these compartments (Fig. 5*A*). However, in transfected cells we did observe co-localization of CTLA-4 with LAMP-1, suggesting traffic to lysosomal compartments (Fig. 5*B*). Despite limited colocalization, the inhibition of protein synthesis by CHX revealed a rapid loss of total CTLA-4 protein when analyzed by flow cytometry (Fig. 5*C*). Furthermore, loss of CTLA-4 was prevented by the addition of the lysosomal inhibitor ammonium chloride (NH_4Cl), suggesting that CTLA-4 was being degraded in lysosomes. These results were also consistent with biochemical analysis of CTLA-4 by Western blotting, indicating that CTLA-4 protein was indeed degraded rather than a loss of signal being due to loss of fluorescence (Fig. 5*D*).

Finally, to ensure that the effects of CHX were directly on CTLA-4 degradation rather than loss of other proteins affecting CTLA-4 stability caused by CHX treatment, we prelabeled a pool of CTLA-4 receptors and chased the degradation of this pool by flow cytometry. This demonstrated that the half-life of CTLA-4 was unaltered by CHX treatment and that CTLA-4 was degraded in a NH_4Cl-sensitive manner (Fig. 5*E*). Taken together, these results indicate that the trafficking pool of CTLA-4 is regulated by both recycling and degradation pathways.

Internalization of CTLA-4 Is Not Impaired during T Cell Activation—Having characterized the features of CTLA-4 endocytosis in model systems, we next studied CTLA-4 behav-

ior in T cells. Given the highly endocytic nature of CTLA-4, it has been proposed that endocytosis might be stopped by phosphorylation during T cell activation, allowing CTLA-4 to be stabilized at the cell surface, thereby facilitating interactions with ligands that potentially deliver inhibitory signals. In support of this concept, studies in the presence of the general phosphatase inhibitor pervanadate have shown phosphorylation of CTLA-4 and that direct phosphorylation of YVKM-containing peptides clearly disrupts interactions with AP-2 (18, 21, 22). Nonetheless, the disengagement of AP-2 and disruption of CTLA-4 trafficking in cellular settings has not been established. We, therefore, directly tested whether the constitutive endocytosis of CTLA-4 was disrupted during T cell activation.

We generated human primary T cell blasts and studied the trafficking of CTLA-4 as well as a number of other cell surface proteins by labeling at 37 °C. This revealed that despite activation, CTLA-4 was found predominantly in the characteristic vesicular distribution with very limited cell surface expression in comparison to CD4 (Fig. 6*A*). This phenotype contrasted with that of CD28, which despite staining at 37 °C remained at the cell surface (Fig. 6*B*). Additional stains including the endocytic receptor CD71 and surface protein CD2 also gave the predicted staining patterns using this approach (data not shown). In addition, we labeled activated T cells for surface CTLA-4 followed by staining for clathrin. This revealed that where CTLA-4 was detectable at the cell surface, it was already in close proximity to clathrin, suggesting its continued recruitment to clathrin-coated pits (Fig. 6*C*). Thus simple confocal analysis of CTLA-4 after normal activation did not suggest CTLA-4 being stabilized at the cell surface or disengaged from clathrin pits.

To directly test the trafficking of CTLA-4, we re-stimulated T cell blasts with either PMA plus ionomycin or anti-CD3/anti-CD28 beads and labeled the cycling pool of CTLA-4. Stimulation led to an increase in the cycling pool of CTLA-4 detected by antibody labeling at 37 °C (Fig. 7*A*). However, in a similar manner to previous experiments, when we labeled both cycling and surface CTLA-4, we obtained plots characteristic of endocytic CTLA-4 (Fig. 7*B*) that contrasted with CD28 which showed the linear relationship characteristic of a cell surface receptor. Notably, these data were similar to those from CHO models obtained in Fig. 1. When we calculated the proportion of CTLA-4 that remained at the cell surface as a fraction of cycling at the membrane at 37 °C, we observed a decrease in this ratio, indicating that CTLA-4 was, if anything, more efficiently internalized (Fig. 7*C*). Therefore, although the cycling pool of CTLA-4 increased upon T cell activation, the relationship between surface and cycling CTLA-4 remained characteristic of an endocytic protein. These results were confirmed using confocal microscopy, which revealed that even after T cell stimulation the pool of trafficking CTLA-4 was predominantly vesicular and substantially in excess of CTLA-4 detected at the cell surface (Fig. 7*D*). Together, these data provide evidence that in activated human T cells, endocytosis of CTLA-4 continues despite a stimulated increase in trafficking.

Activation of T cells has two effects on CTLA-4 expression; an increase in total CTLA-4 via transcriptional up-regulation and an accompanying increase in protein trafficking. To study

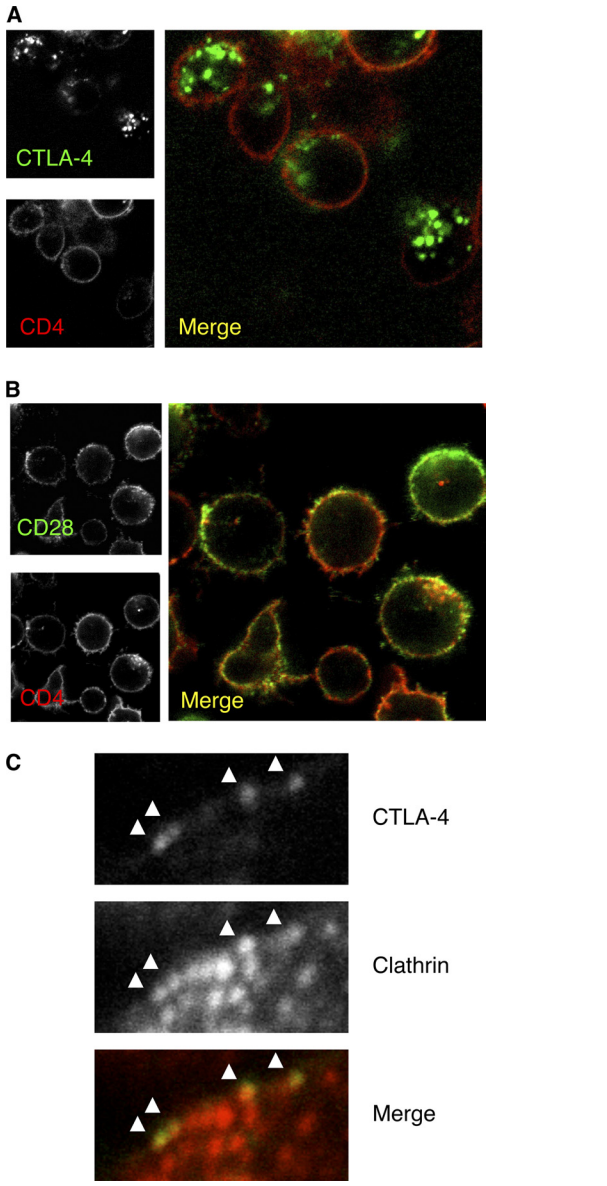

FIGURE 6. **CTLA-4 remains predominantly intracellular in activated T cells.** *A*, human CD4+ T cell blasts were generated using anti-CD3 anti-CD28 beads for 4 days. Cells were then incubated with anti-CD4 FITC and PE-conjugated antibody against CTLA-4 (*A*) or CD28 (*B*) at 37 °C for 60 min and visualized by confocal microscopy. *C*, surface CTLA-4 was detected at 4 °C. Cells were then fixed and permeabilized and stained for clathrin and analyzed by confocal microscopy.

CTLA-4 trafficking in isolation, we also generated Jurkat cells that constitutively expressed CTLA-4 under a CMV promoter. Stimulation of these cells showed a similar increase in labeling of cycling CTLA-4 at 37 °C (Fig. 8*A*). Moreover, when we compared total CTLA-4 with cycling CTLA-4, we observed a clear increase in the cycling label after stimulation. Furthermore, the more linear relationship between cycling and total CTLA-4 after stimulation indicated that more of the total pool of CTLA-4 protein trafficked via the plasma membrane (Fig. 8, *B* and *C*). Nonetheless, when we measured cycling CTLA-4 against cell surface CTLA-4, we again observed the characteristic non-linear relationship typical of an endocytic protein (Fig. 8*D*), indicating that CTLA-4 was not stabilized at the plasma membrane after stimulation. Importantly, after stimulation, a

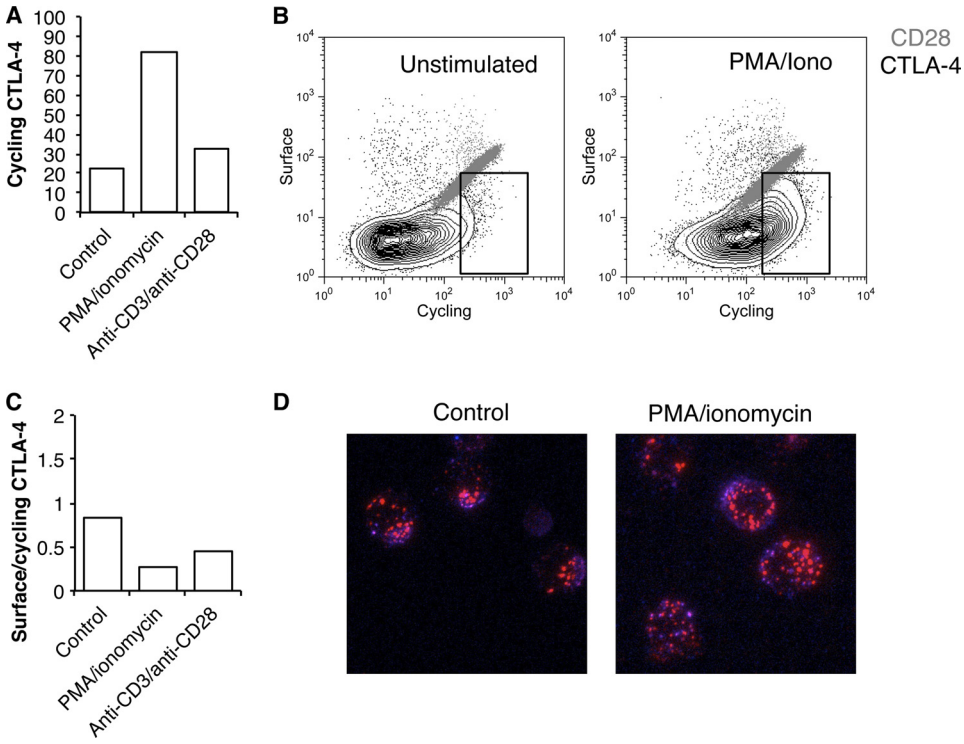

FIGURE 7. **Stimulation of T cell blasts leads to a mobilization but not stabilization of CTLA-4 at the cell surface.** *A*, human CD4+ T cell blasts were generated using anti-CD3 anti-CD28 beads for 4 days. Cells were then isolated and re-stimulated with PMA+ ionomycin or fresh anti-CD3 anti-CD28 beads for 3 h at 37 °C in the presence of anti-CTLA-4 PE before analysis by flow cytometry. *B*, T cell blasts were re-stimulated as in *A* in the presence of anti-CTLA-4 PE or anti-CD28 PE at 37 °C. Cells were then placed on ice, and the remaining surface receptors were labeled by incubation with Alexa647-conjugated anti-mouse secondary antibody. Cells were analyzed by flow cytometry. The *boxed area* indicates an increase in CTLA-4 labeling due to stimulation. *C*, the ratio of surface to labeled fluorescence for cells labeled in *B* is plotted. *D*, cells stained for CTLA-4 as in *B* were fixed and then visualized by confocal microscopy for 37 °C staining (*red*) and surface staining (*blue*).

clear increase in CTLA-4 cycling was detected due to mobilization from intracellular compartments resulting in increased surface detection. However, the ratio between surface and cycling CTLA-4 remained unaltered (Fig. 8*E*). Thus, whereas CTLA-4 traffic to the plasma membrane is increased after stimulation, no change in endocytosis is apparent.

DISCUSSION

CTLA-4 plays a critical, non-redundant role in controlling T cell immune responses, and numerous functional and genetic studies implicate CTLA-4 in the control of autoimmunity (6, 28). Several mechanisms have been proposed for the function of CTLA-4, but these are still debated (5, 7, 29). Nonetheless, the specific subcellular distribution and control of CTLA-4 intracellular trafficking is likely to be of central importance in influencing function and holds implications for its potential mechanisms of action. We have, therefore, characterized in more detail the behavior of CTLA-4 in a number of cellular systems including CHO cells, Jurkat cells, and T cell blasts. In all of these systems we have observed comparable trafficking behavior consistent with the fact that the endocytic machinery is highly conserved between species and ubiquitously expressed. Accordingly, it is clear that CTLA-4 is constitutively turned over at the plasma membrane in the absence of ligand binding in a manner controlled by its highly conserved cytoplasmic domain.

Endocytic receptors can utilize a variety of mechanisms to achieve internalization that may or may not depend on clathrin and dynamin (30). Here we have demonstrated CTLA-4 utilizes an endocytic pathway controlled by both clathrin and dynamin. Studies of the $YXX\phi$ motif within the CTLA-4 C terminus have been widely performed and provide robust evidence of the influence of this motif on CTLA-4 expression. Truncations and mutations affecting this motif result in increased CTLA-4 surface expression by profoundly impairing the internalization rate. In addition to the well established YVKM motif, recent studies have suggested that an additional motif, $YXXX\phi N$, may also be present in CTLA-4 and interact with $\mu 2$ at a site distinct from the YVKM motif (31). Together, these data now provide further detail to the pathway of CTLA-4 endocytosis.

A major issue pertaining to the function of CTLA-4 is how its highly endocytic nature permits interactions with cell surface ligands on APCs. Several previous studies have suggested that phosphorylation of CTLA-4 at the tyrosine residue in its $YXX\phi$ motif has the potential to stabilize CTLA-4 at the plasma membrane by blocking the interaction with AP-2 (18, 20). Given the low surface expression of CTLA-4, this might be important to allow generation of inhibitory signals to the T cell or possibly reverse signal via its ligands (32). Evidence exists that when CTLA-4 is deliberately phosphorylated, interactions with AP-2 are inhibited (18, 20, 21, 33). However, in these systems the phosphorylation of CTLA-4 is driven, for example, by *in vitro* phosphorylation of peptides, overexpression of src kinases, or by the addition of the phosphatase inhibitor pervanadate. Currently, two pieces of evidence are still lacking; 1) whether

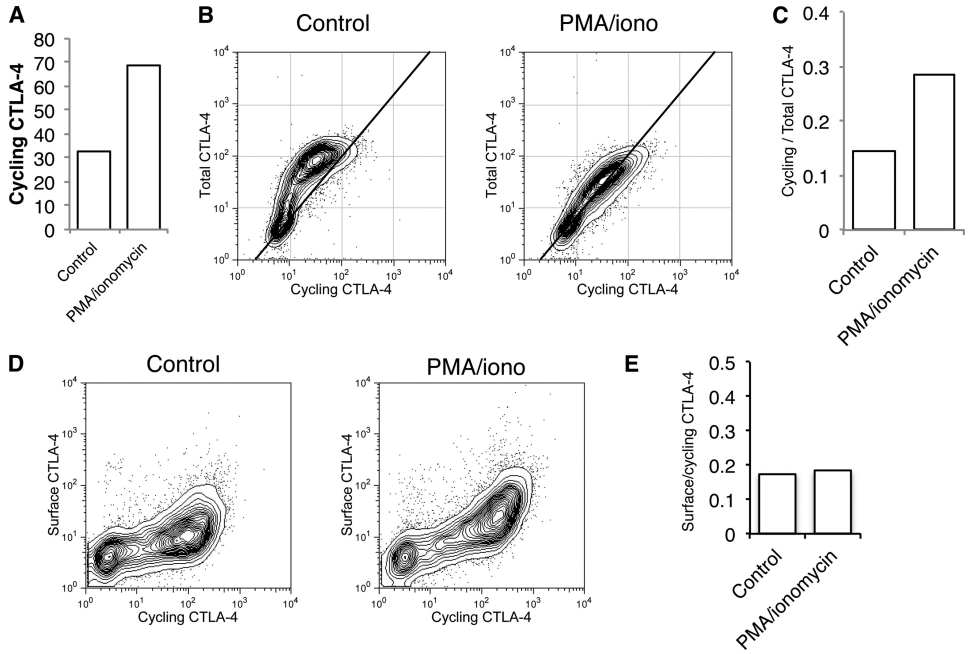

FIGURE 8. **Stimulation increases trafficking of CTLA-4 in the absence of increased synthesis.** *A*, CTLA-4-expressing Jurkat cells were labeled at 37 °C with anti-CTLA-4 PE for 1 h after stimulation with PMA/ionomycin and analyzed by flow cytometry. *B*, Jurkat cells were labeled at 37 °C with anti-CTLA-4 PE in the presence or absence of PMA/ionomycin for 60 min (*cycling CTLA-4*). Cells were then fixed, and total CTLA-4 was stained with a goat anti-CTLA-4 C-terminal antibody followed by Alexa633 anti-goat secondary and analyzed by flow cytometry. *C*, shown is the ratio of labeled to total CTLA-4 for cells, stained as in B. *D*, Jurkat cells were labeled at 37 °C with anti-CTLA-4 PE in the presence or absence of PMA/ionomycin for 60 min (cycling CTLA-4). Cells were then placed on ice, and the remaining surface receptors were labeled by incubation with Alexa647-conjugated anti-mouse secondary antibody (surface CTLA-4). Cells were analyzed by flow cytometry. *E*, shown is the ratio of surface to cycling CTLA-4 fluorescence for cells labeled in *D*.

CTLA-4 is phosphorylated in normal T cells undergoing physiological stimulation and 2) whether endocytosis of CTLA-4 is inhibited during stimulation. In our studies of human T cells we have addressed this latter question. During T cell stimulation, we did observe an increase in trafficking of CTLA-4 to the plasma membrane and consequently an increase in the amount of CTLA-4 on the cell surface. This is expected given the increase in delivery and assuming no accompanying change in the rate of endocytosis. Such increases at the plasma membrane are consistent with previous observations (10, 17). However, when we measured the ratio of CTLA-4 at the plasma membrane relative to that internalized, we found no evidence of increased CTLA-4 stability at the plasma membrane. Furthermore, confocal images of activated T cells at 37 °C did not show cell surface accumulation of CTLA-4 after stimulation despite the considerable amounts of CTLA-4 being labeled, which contrasted with several known surface receptors. Thus, under the conditions tested here, we find no evidence that endocytosis of CTLA-4 is disrupted during T cell activation.

Once internalized, the fate of CTLA-4 is poorly understood. Our studies provide direct evidence that once internalized, CTLA-4 undergoes recycling to the cell surface. The purpose of recycling of CTLA-4 is unknown; however, recently we have shown that one function of CTLA-4 is its ability to remove ligands from antigen-presenting cells (8). One interesting possibility, therefore, is that by recycling CTLA-4, T cells could allow molecules to be efficiently reused for ligand depletion. Thus one might envisage that CTLA-4 could act like a molecular pump capable of removing ligands from APCs. Moreover, in principle, the ability of T cells to remove ligands would not be simply limited by the level of CTLA-4 expression but also by cell-cell contact time and the rate at which CTLA-4 can be recycled. Thus recycling CTLA-4 may enhance the efficiency with which CTLA-4 can remove ligands from the synapse between T cell and APC.

In keeping with other studies, we also observed that CTLA-4 is effectively targeted for degradation in lysosomal compartments (13, 17, 34). The detection of co-localization of CTLA-4 with lysosomal compartments using antibody markers has generally been variable (15, 16). This likely reflects the fact that CTLA-4 is rather rapidly degraded, and consequently co-localization is difficult to observe. The purpose of CTLA-4 degradation is also unclear. Degradation has previously been suggested to be a mechanism by which cells can control their overall level of CTLA-4 (34). An additional possibility, however, is that the targeting of CTLA-4 to lysosomes may be important to its function. Here again our recent studies on trans-endocytosis provide an interesting change in perspective (8). We observed that captured ligands were effectively degraded in lysosomes and that inhibitors such as bafilomycin and ammonium chloride prevented degradation. Thus for this function, trafficking of CTLA-4 to lysosomes would be required to effectively dispose of captured ligands. Furthermore, we also observed that the ability to degrade ligand and the degradation of CTLA-4 itself might be uncoupled such that CTLA-4 may be able to deliver ligands to lysosomes and still be able to recycle itself. Thus the trafficking itinerary of CTLA-4, encoded by its highly conserved cytoplasmic domain, appears well suited for the function of capturing and degrading ligands in lysosomes, and further detailed studies of this process should prove useful.

Taken together the data presented here provide a more detailed and comprehensive perspective on the nature of CTLA-4 trafficking and its relevance to function. We propose that CTLA-4 does not exist as a stable plasma membrane receptor and that during T cell activation CTLA-4 continues to endocytose. Furthermore, its trafficking itinerary, which includes recycling endosomes and lysosomes, could be a potentially important aspect of its molecular function. Thus the balance of these various outcomes will likely control the efficiency of CTLA-4 function. Accordingly, genetic variations that affect these aspects of protein trafficking may well have unexpected influence on susceptibility to autoimmunity by affecting CTLA-4 function. Ultimately, understanding pathways that influence CTLA-4 expression patterns is likely to be of importance in designing novel therapies for autoimmunity and cancer.

REFERENCES

1. Tivol, E. A., Borriello, F., Schweitzer, A. N., Lynch, W. P., Bluestone, J. A., and Sharpe, A. H. (1995) Loss of CTLA-4 leads to massive lymphoproliferation and fatal multiorgan tissue destruction, revealing a critical negative regulatory role of CTLA-4. *Immunity* **3,** 541–547
2. Waterhouse, P., Penninger, J. M., Timms, E., Wakeham, A., Shahinian, A., Lee, K. P., Thompson, C. B., Griesser, H., and Mak, T. W. (1995) Lymphoproliferative disorders with early lethality in mice deficient in Ctla-4. *Science* **270,** 985–988
3. Sansom, D. M. (2000) CD28, CTLA-4, and their ligands. Who does what and to whom? *Immunology* **101,** 169–177
4. Teft, W. A., Kirchhof, M. G., and Madrenas, J. (2006) A molecular perspective of CTLA-4 function. *Annu. Rev. Immunol.* **24,** 65–97
5. Rudd, C. E. (2008) The reverse stop-signal model for CTLA4 function. *Nat. Rev. Immunol.* **8,** 153–160
6. Wing, K., Yamaguchi, T., and Sakaguchi, S. (2011) Cell-autonomous and -non-autonomous roles of CTLA-4 in immune regulation. *Trends Immunol.* **32,** 428–433
7. Walker, L. S., and Sansom, D. M. (2011) The emerging role of CTLA4 as a cell-extrinsic regulator of T cell responses. *Nat. Rev. Immunol.* **11,** 852–863
8. Qureshi, O. S., Zheng, Y., Nakamura, K., Attridge, K., Manzotti, C., Schmidt, E. M., Baker, J., Jeffery, L. E., Kaur, S., Briggs, Z., Hou, T. Z., Futter, C. E., Anderson, G., Walker, L. S., and Sansom, D. M. (2011) Trans-endocytosis of CD80 and CD86. A molecular basis for the cell-extrinsic function of CTLA-4. *Science* **332,** 600–603
9. Chuang, E., Alegre, M. L., Duckett, C. S., Noel, P. J., Vander Heiden, M. G., and Thompson, C. B. (1997) Interaction of CTLA-4 with the clathrin-associated protein AP50 results in ligand-independent endocytosis that limits cell surface expression. *J. Immunol.* **159,** 144–151
10. Linsley, P. S., Bradshaw, J., Greene, J., Peach, R., Bennett, K. L., and Mittler, R. S. (1996) Intracellular trafficking of CTLA-4 and focal localization toward sites of TCR engagement. *Immunity* **4,** 535–543
11. Leung, H. T., Bradshaw, J., Cleaveland, J. S., and Linsley, P. S. (1995) Cytotoxic T lymphocyte-associated molecule-4, a high avidity receptor for CD80 and CD86, contains an intracellular localization motif in its cytoplasmic tail. *J. Biol. Chem.* **270,** 25107–25114
12. Alegre, M. L., Shiels, H., Thompson, C. B., and Gajewski, T. F. (1998) Expression and function of CTLA-4 in Th1 and Th2 cells. *J. Immunol.* **161,** 3347–3356
13. Iida, T., Ohno, H., Nakaseko, C., Sakuma, M., Takeda-Ezaki, M., Arase, H., Kominami, E., Fujisawa, T., and Saito, T. (2000) Regulation of cell surface expression of CTLA-4 by secretion of CTLA-4-containing lysosomes upon activation of CD4+ T cells. *J. Immunol.* **165,** 5062–5068
14. Barrat, F. J., Le Deist, F., Benkerrou, M., Bousso, P., Feldmann, J., Fischer, A., and de Saint Basile, G. (1999) Defective CTLA-4 cycling pathway in Chediak-Higashi syndrome. A possible mechanism for deregulation of T lymphocyte activation. *Proc. Natl. Acad. Sci. U.S.A.* **96,** 8645–8650
15. Mead, K. I., Zheng, Y., Manzotti, C. N., Perry, L. C., Liu, M. K., Burke, F., Powner, D. J., Wakelam, M. J., and Sansom, D. M. (2005) Exocytosis of CTLA-4 is dependent on phospholipase D and ADP ribosylation factor-1 and stimulated during activation of regulatory T cells. *J. Immunol.* **174,** 4803–4811
16. Catalfamo, M., Tai, X., Karpova, T., McNally, J., and Henkart, P. A. (2008) TcR-induced regulated secretion leads to surface expression of CTLA-4 in CD4+CD25+ T cells. *Immunology* **125,** 70–79
17. Egen, J. G., and Allison, J. P. (2002) Cytotoxic T lymphocyte antigen-4 accumulation in the immunological synapse is regulated by TCR signal strength. *Immunity* **16,** 23–35
18. Bradshaw, J. D., Lu, P., Leytze, G., Rodgers, J., Schieven, G. L., Bennett, K. L., Linsley, P. S., and Kurtz, S. E. (1997) Interaction of the cytoplasmic tail of CTLA-4 (CD152) with a clathrin-associated protein is negatively regulated by tyrosine phosphorylation. *Biochemistry* **36,** 15975–15982
19. Miyatake, S., Nakaseko, C., Umemori, H., Yamamoto, T., and Saito, T. (1998) Src family tyrosine kinases associate with and phosphorylate CTLA-4 (CD152). *Biochem. Biophys. Res. Commun.* **249,** 444–448
20. Chuang, E., Lee, K. M., Robbins, M. D., Duerr, J. M., Alegre, M. L., Hambor, J. E., Neveu, M. J., Bluestone, J. A., and Thompson, C. B. (1999) Regulation of cytotoxic T lymphocyte-associated molecule-4 by Src kinases. *J. Immunol.* **162,** 1270–1277
21. Shiratori, T., Miyatake, S., Ohno, H., Nakaseko, C., Isono, K., Bonifacino, J. S., and Saito, T. (1997) Tyrosine phosphorylation controls internalization of CTLA-4 by regulating its interaction with clathrin-associated adaptor complex AP-2. *Immunity* **6,** 583–589
22. Follows, E. R., McPheat, J. C., Minshull, C., Moore, N. C., Pauptit, R. A., Rowsell, S., Stacey, C. L., Stanway, J. J., Taylor, I. W., and Abbott, W. M. (2001) Study of the interaction of the medium chain μ2 subunit of the clathrin-associated adapter protein complex 2 with cytotoxic T-lymphocyte antigen 4 and CD28. *Biochem. J.* **359,** 427–434
23. Benmerah, A., Bayrou, M., Cerf-Bensussan, N., and Dautry-Varsat, A. (1999) Inhibition of clathrin-coated pit assembly by an Eps15 mutant. *J. Cell Sci.* **112,** 1303–1311
24. Granseth, B., Odermatt, B., Royle, S. J., and Lagnado, L. (2006) Clathrin-mediated endocytosis is the dominant mechanism of vesicle retrieval at hippocampal synapses. *Neuron* **51,** 773–786
25. Sharma, D. K., Choudhury, A., Singh, R. D., Wheatley, C. L., Marks, D. L., and Pagano, R. E. (2003) Glycosphingolipids internalized via caveolar-related endocytosis rapidly merge with the clathrin pathway in early endosomes and form microdomains for recycling. *J. Biol. Chem.* **278,** 7564–7572
26. Choudhury, A., Dominguez, M., Puri, V., Sharma, D. K., Narita, K., Wheatley, C. L., Marks, D. L., and Pagano, R. E. (2002) Rab proteins mediate Golgi transport of caveola-internalized glycosphingolipids and correct lipid trafficking in Niemann-Pick C cells. *J. Clin. Invest.* **109,** 1541–1550
27. Macia, E., Ehrlich, M., Massol, R., Boucrot, E., Brunner, C., and Kirchhausen, T. (2006) Dynasore, a cell-permeable inhibitor of dynamin. *Dev. Cell* **10,** 839–850
28. Gough, S. C., Walker, L. S., and Sansom, D. M. (2005) CTLA4 gene polymorphism and autoimmunity. *Immunol. Rev.* **204,** 102–115
29. Sansom, D. M., and Walker, L. S. (2006) The role of CD28 and cytotoxic T-lymphocyte antigen-4 (CTLA-4) in regulatory T-cell biology. *Immunol. Rev.* **212,** 131–148
30. Doherty, G. J., and McMahon, H. T. (2009) Mechanisms of endocytosis. *Ann. Rev. Biochem.* **78,** 857–902
31. Kozik, P., Francis, R. W., Seaman, M. N., and Robinson, M. S. (2010) A screen for endocytic motifs. *Traffic* **11,** 843–855
32. Fallarino, F., Grohmann, U., Hwang, K. W., Orabona, C., Vacca, C., Bianchi, R., Belladonna, M. L., Fioretti, M. C., Alegre, M. L., and Puccetti, P. (2003) Modulation of tryptophan catabolism by regulatory T cells. *Nat. Immunol.* **4,** 1206–1212
33. Hu, H., Rudd, C. E., and Schneider, H. (2001) Src kinases Fyn and Lck facilitate the accumulation of phosphorylated CTLA-4 and its association with PI-3 kinase in intracellular compartments of T-cells. *Biochem. Biophys. Res. Commun.* **288,** 573–578
34. Schneider, H., Martin, M., Agarraberes, F. A., Yin, L., Rapoport, I., Kirchhausen, T., and Rudd, C. E. (1999) Cytolytic T lymphocyte-associated antigen-4 and the TCRζ/CD3 complex, but not CD28, interact with clathrin adaptor complexes AP-1 and AP-2. *J. Immunol.* **163,** 1868–1879